



# The role of both intercalation and groove binding at AT-rich DNA regions in the interaction process of a dinuclear Cu(I) complex probed by spectroscopic and simulation analysis

Nahid Shahabadi<sup>a,\*</sup>, Farshad Shiri<sup>a</sup>, Saba Hadidi<sup>a</sup>, Kaveh Farshadfar<sup>b</sup>, Maryam Darbemamieh<sup>c</sup>, S. Mark Roe<sup>d</sup>

<sup>a</sup> Department of Inorganic Chemistry, Faculty of Chemistry, Razi University, Kermanshah, Iran

<sup>b</sup> Department of Chemistry, Islamic Azad University, Central Tehran Branch, Poonak, Tehran 1469669191, Iran

<sup>c</sup> Department of Plant Protection, Faculty of Agriculture, Campus of Agriculture and Natural Resources, Razi University, Kermanshah, Iran

<sup>d</sup> Department of Chemistry, School of Life Sciences, University of Sussex, Brighton, BN1 9QJ, UK

## ARTICLE INFO

### Article history:

Received 25 February 2021

Revised 17 April 2021

Accepted 21 April 2021

Available online 24 April 2021

### Keywords:

Dinuclear Cu(I) complex

DNA binding

In vitro evaluation

Spectroscopic techniques

Docking simulation

Cytotoxicity study

## ABSTRACT

In this research paper, the synthesis process and characterization of a dinuclear Cu(I) phosphine complex, as well as spectroscopic and simulation analysis of its interaction with DNA helix, are presented. The monoclinic phase  $[\text{Cu}(\text{PPh}_3)(\text{L}_{0.5})(\text{I})]_2$  with a tetrahedral molecular geometry was elucidated based on X-ray single-crystal diffraction data. The significant association constant ( $6.88 \times 10^5$ ) and remarkable hyperchromism as obtained from UV-Visible spectra indicated a high binding affinity of the Cu(I) complex for DNA, which is in accordance with both intercalation and groove binding modes. The results of competitive fluorescence experiments along with molecular docking simulation proved that the planar part of the complex can insert into the core of adenine nucleobases and compete with methylene blue for the intercalative binding sites, while the bulky substituent binds in the minor groove of DNA via replacement of Hoechst molecules at A-T rich regions. According to thermodynamic parameters (the negative values of  $\Delta H^\circ$  and  $\Delta S^\circ$ ), it is quite clear that the interaction process is enthalpy-favored while disfavored by entropy and van der Waals and hydrophobic forces play a major role in stabilization of right-handed B-DNA form during the interaction, as shown in the circular dichroism spectra. Based on the above findings partial intercalation mode at A-T rich region of DNA was proposed. The cytotoxicity and apoptosis results on MCF-7 cell line indicated positive effect of the Cu(I) complex in controlling growth and viability of breast cancer more than cisplatin.

© 2021 Elsevier B.V. All rights reserved.

## 1. Introduction

Copper as a crucial trace element is essential for all living organisms and cell metabolism [1]. It is needed for the proper function of enzyme systems, most notably cytochrome oxidase, respiration, DNA synthesis, ascorbate oxidase, energy production, and metabolism [2,3]. Nevertheless, copper can also function as an essential cofactor in tumor angiogenesis processes [4]. Consistently, major levels of copper have been found in many human cancer types, including breast, lung, brain, liver, colon, prostate, and bladder cancers [5]. On this base, the use of copper chelators is known as

anti-angiogenic molecules in several types of cancers [6–9]. In this regard, recent research studies have provided evidence that copper complexes containing chelating phosphines act as a proteasome inhibitor and apoptosis inducer in different human cancer cells [10,11]. Hydrophilic phosphine ligands are also utilized as a strategy to acquire easy membrane penetrating drugs [12]. The antiproliferative activity of a copper(I) phosphine complex  $[\text{Cu}(\text{thp})_4][\text{PF}_6]$  (CP) against human solid tumors with poor effects on non-tumor cells is a promising point for considering these compounds as novel anticancer agents [13,14]. CP demonstrated 40-fold more cytotoxic potency than cisplatin and it was also able to overcome multi-drug resistance problems [13]. The cytotoxic activities of copper(I) phosphine complexes may be correlated to their different mode of action from that of cisplatin for damaging DNA as the main molecular target for anticancer drugs [15–17]. Mechanistic studies

Abbreviations: CT-DNA, Calf thymus DNA; MB, Methylene blue; CD, Circular dichroism.

\* Corresponding author.

E-mail address: [n.shahabadi@razi.ac.ir](mailto:n.shahabadi@razi.ac.ir) (N. Shahabadi).

proved that cisplatin binds covalently to DNA [18,19] while copper complexes generally interact with DNA via non-covalent interactions and cause stronger damage to DNA [12,20–23]. Based on the results obtained, DNA intercalators and groove binders show promising anticancer effect with high binding constant on  $10^5$ – $10^8$   $M^{-1}$  order of magnitude [24–26], while covalent DNA binders such as cisplatin have lower binding constant in the order of  $10^4$   $M^{-1}$  [19,27]. On the other hand, because of the low specificity of DNA recognition and the omnipresence of its potential binding sites, cisplatin is not a region-specific anticancer agent [28]. Damage to DNA in various domains does not show a consistent relationship with cytotoxic activities of anticancer drugs contrary to what has been observed in region-specific DNA damage. Thus, specific DNA targeting offers the potential to improve antitumor activities and treatment selectivity against tumors versus normal cells. Understanding how drugs interact with DNA and how induce DNA damage can be helpful to design more efficient and specifically targeted therapeutics, with lower side effects [24,29]. Hence, with knowledge of the importance of the subject, we sought to design a dinuclear Cu(I) complex containing chelating phosphine ligand with the ability to interact with DNA in a remarkably specific way through non-covalent interactions.

## 2. Experimental

### 2.1. Materials

All materials including metal ion, buffers, nucleic acid, and other chemicals for synthesis process and DNA interaction experiments were of analytical reagent grade and used without purification. Doubly distilled water was applied to prepare Tris-HCl buffer and all aqueous stock solutions. A solution of  $8.6 \times 10^{-3}$  mol/L of Calf thymus DNA (CT-DNA) in Tris-HCl buffer (pH 7.4) was used as a stock solution of DNA and its protein purity was checked by monitoring the ratio of  $A_{260}/A_{280} > 1.80$  [30]. All spectroscopic studies were carried out in Tris-HCl buffer (50 mM, pH 7.4) including 0.05% DMSO and 0.1% Ethanol.

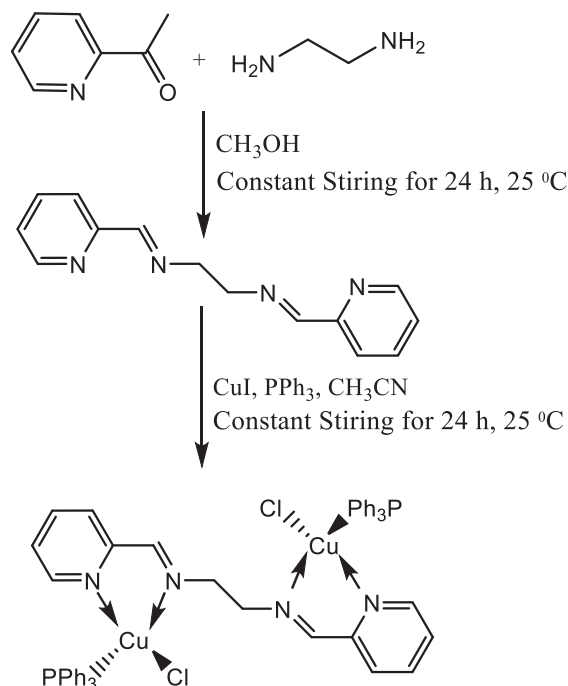
### 2.2. Synthesis of the Cu(I) complex

The synthesis of the Cu(I) complex  $[Cu(PPh_3)(L_{0.5})(I)]_2$  was performed according to previously published methods of our group [31,32]. The ligand N,N'-Bis(2-pyridylmethylene)ethylenediamine<sup>1</sup> (L) was prepared by mixing equivalent amounts of 1 mmol pyridine-2-carbaldehyde and 1 mmol ethane-1,2-diamine in methanol solution under constant stirring for 24 h [33]. By adding 0.2 mmol of the synthesized ligand solution to a mixture of 0.2 mmol of  $PPh_3$  and 0.2 mmol of Cu(I) iodide in acetonitrile under constant stirring for 24 h, the formed orange-colored complex was filtered off (yield: 92%) (Scheme 1). Slow diffusion of diethyl ether into the filtered solutions yielded orange needle crystal.

### 2.3. DNA-binding procedures

#### 2.3.1. UV-Visible absorption measurements

The UV-Visible absorption spectra of DNA (2 mL,  $1.45 \times 10^{-5}$  mol/L in Tris-HCl pH = 7.4) by increasing the concentration of the Cu(I) complex from 0 to  $4.69 \times 10^{-6}$  mol/L were recorded in the wavelength range of 200–400 nm on a Nordantec T80 UV-Visible spectrophotometer.



Scheme 1. Schematic view of the compounds and synthesis processes.

#### 2.3.2. Competitive fluorescence analysis

All fluorescence spectra were performed on JASCO spectrofluorimeter Model FP-6200 equipped with a thermostated bath, using a 1.0 cm quartz cell. 2 mL solution of DNA-Hoechst conjugate ( $C_{DNA} = 1.18 \times 10^{-3}$  mol/L and  $C_{Hoechst} = 5 \times 10^{-6}$  mol/L in Tris-HCl pH = 7.4) was titrated by increasing concentration of the Cu(I) complex to  $1.12 \times 10^{-4}$  mol/L at different temperatures (288, 293, 298, and 303 K) in the wavelength range of 350–550 nm with exciting wavelength at 340 nm. The competitive interaction between methylene blue (MB) and the Cu(I) complex was carried out by the addition of increasing amounts of the Cu(I) complex (from 0 to  $2.33 \times 10^{-4}$  mol/L) against a constant amount of the probes ( $5 \times 10^{-6}$  mol/L) and DNA ( $1.96 \times 10^{-4}$  mol/L) at 288 K in the wavelength range of 630–730 nm with exciting wavelength at 630 nm. All fluorescence intensities were corrected for absorption of the exciting light and reabsorption of the emitted light to decrease the inner filter effect using the following relationship (Eq. (1)) [34]:

$$F_{cor} = F_{obs} \times e^{A_{ex} + A_{em}/2} \quad (1)$$

here  $F_{cor}$  and  $F_{obs}$  are the corrected and observed fluorescence intensities, respectively and  $A_{ex}$  and  $A_{em}$  are the absorption of the system at the excitation and the emission wavelength, respectively.

#### 2.3.3. Circular dichroism spectroscopy

Circular dichroism spectra of DNA ( $2.15 \times 10^{-5}$  mol/L in Tris-HCl pH = 7.4) in the presence of the Cu(I) complex ( $1.81 \times 10^{-6}$  mol/L) were made on a JASCO spectropolarimeter Model J-810 using a 1.0 cm quartz cell. The CD spectra were recorded at room temperature in a wavelength range of 200–300 nm.

#### 2.3.4. Statistical analysis

All assays were executed in triplicate and the standard deviation was calculated by the following equation (Eq. (2)) as the square root of variance with determining each data point's deviation relative to the mean.

<sup>1</sup> ChemSpider ID 92,443

$$\text{Standard Deviation} = \sqrt{\left[\sum_{i=1}^n (xi - \bar{x})^2 / (n - 1)\right]} \quad (2)$$

where  $x_i$  is value of the  $i$ th point in the data set,  $\bar{x}$  represents the mean value of the data set and the number of data points in the data set has been shown with  $n$ .

#### 2.4. Molecular docking simulation

The open-source AutoDock Vina (version 1.1.2) [35] and MGL tools 1.5.6 [36,37] were used to perform docking simulations. The partial charges of Gasteiger and polar hydrogens were added to the Cu(I) complex and all rotatable bonds were defined. The B-DNA sequence CGCGAATTCGCG/CGCGAATTCGCG was selected from the Protein Data Bank (PDB ID: 1g3x) [38], because it has a good structure resolution and closest sequence identity to the parent AA/TT base for drug binding site in this work. Moreover, the natural ligand present in the structure is considered as the possible binding site for this structure. The DNA 3D structure and the resultant docked were visualized by performing the visual molecular dynamics, VMD. The DNA was enclosed in a box with the number of points in  $x$ ,  $y$ , and  $z$  dimensions of 20, 40, and 20 and center grid box of 57.64, 49.00, and 58.63 with a grid spacing of 1.00 Å. The docking calculation was performed using the Lamarckian genetic algorithm (LGA) [39].

#### 2.5. Cell culture

The effects of the Cu(I) complex on human breast cancer cells (MCF-7) and human umbilical venous endothelial cells (HUVEC) were evaluated. The cell lines were routinely cultured on the DMEM medium supplemented with fetal bovine serum and antibiotics. Proliferated cells were frozen for later use. The cells were seeded in 96-well cell culture plate at a density of  $1 \times 10^4$  cells per well. The plate transferred to an incubator with 37 °C temperature, 95% relative humidity and 5% CO<sub>2</sub>. After 24 h, the Cu(I) complex and cisplatin with different concentrations (20, 40, 80, and 160 µg/mL), added on DMEM culture medium supplemented with fetal bovine serum and penicillin/streptomycin as antibiotics. The Cu(I) complex-free group considered as control. After 72 h of incubation with the Cu(I) complex and cisplatin, about 20 µL of MTT solution at a concentration of 5 mg/mL DPBS added to each well and, finally, incubated in a 37 °C incubator for 4 h. At the end of the incubation period, the medium was removed and 100 µL of DMSO were added to each well then reading was performed at 570 nm with the ELISA reader. The results analyzed by SPSS software using completely random design and then means compared.

##### 2.5.1. Investigation of apoptosis by acridin orange-ethidium bromide dye

For this purpose, cells seeded on a 24-well plate and treated with different concentrations of the Cu(I) complex and cisplatin (20, 40, 80, and 160 µg/mL). Passing 72 h, supernatants removed and each well was washed with DPBS solution that being removed later. Then, paraformaldehyde solution was added to it for 15–20 min. Fixing solution was removed and re-washed with DPBS. Finally, Ethidium bromide and acridine orange (1:1) dye were added to each well under dark condition. Cells were photographed and evaluated under a fluorescent microscope.

### 3. Results and discussion

#### 3.1. Single crystal X-ray structure determination

The molecular structure of the synthesized complex [Cu(PPh<sub>3</sub>)<sub>2</sub>(L<sub>0.5</sub>)(I)]<sub>2</sub> (L = N,N'-Bis(2-pyridylmethylene)ethylenediamine) is

displayed in Fig. 1. The X-ray analysis revealed that the Cu(I) complex crystallized in the monoclinic space group P-2<sub>1</sub>/n. The L ligand binds to two copper centers in a bidentate chelating fashion through N1 and N2 to Cu1 on side A and N3 and N4 to Cu2 on side B. The two remaining coordination sites were occupied by PPh<sub>3</sub> and iodide ligands. As evidence, the differences in similar angles and bond lengths in two independent molecule parts are very small. With no significant intermolecular interactions, the molecules are further linked to each other as long as πPPh<sub>3</sub>-πPPh<sub>3</sub> and πPPh<sub>3</sub>-πpy to generate 3D network. Details of the crystallographic data and structure refinement parameters for the synthesized complex are presented in Table 1.

#### 3.2. DNA binding studies

##### 3.2.1. UV-Visible absorption spectroscopy

The preliminary invitro evaluation of binding mode and binding strength of the Cu(I) complex to DNA helix has been performed through spectrophotometric titrations by following the changes in absorbance values and the positions of the absorption band of CT-DNA. Equal aliquots of the Cu(I) complex stock solution were added to both DNA and reference solutions to eliminate the effect of the Cu(I) complex absorbance (Fig. 2A). By increasing the Cu(I) complex concentration, the maximum absorption of DNA helix at 260 nm represents a hyperchromism without any wavelength shift, demonstrating that the Cu(I) complex has strong interaction with DNA (Fig. 2B). The resulted hyperchromism might come from π-π stacking interaction between the DNA-base pairs and the aromatic chromophores in the Cu(I) complex structure along with the separation of DNA strands [44–46].

To determine the binding constant ( $K_b$ ) the UV-Visible data were analyzed based on the following equation (Eq. (3)) [47]:

$$1/(A - A_0) = 1/(A_\infty - A_0) + 1/K_b(A_\infty - A_0) \times 1/[\text{Complex}] \quad (3)$$

here  $A_0$  represents the absorbance of DNA at 260 nm in the absence of the Cu(I) complex,  $A_\infty$  shows the final absorbance of the Cu(I) complex-DNA conjugate, and  $A$  is in accordance with the observed absorbance at different complex concentrations. By the plotting of  $1/(A - A_0)$  versus  $1/[\text{Complex}]$ , the interaction binding constant ( $K_b$ ) of the Cu(I) complex-DNA system was determined to  $6.88 \times 10^5$ , which is indicated that the Cu(I) complex has high DNA binding affinity through insertion of the planer aromatic ring into the DNA base pairs as observed for half sandwich Rh(III) and Ir(III) complexes [24]. The resulted binding constant is also in the range of both the intercalator copper complexes [48–50] and the groove binder cases [51], while higher than anticancer metal complexes such as cisplatin ( $5.51 \times 10^4$  L/mol) [27], and Cu(I) complexes with a phenanthroline-phosphine set of ligands which have binding constants in the range of 6.67 to  $20 \times 10^4$  L/mol [12].

##### 3.2.2. Competitive fluorescence studies

The excitation scanning was performed to determine the fluorescence properties of the Cu(I) complex ( $1 \times 10^{-4}$  mol/L) but no luminescence was observed for the Cu(I) complex upon excitation either in aqueous solution or in the presence of DNA. Therefore, to clarify the portion of the Cu(I) complex interacting with DNA, competitive fluorescence experiments were used for further study of the binding sites with both Hoechst 33,258 as a minor groove binder probe at A-T rich regions [52] and methylene blue probe with DNA intercalation ability [53–55]. In the Hoechst displacement assay (Fig. 3A), it is observed that the fluorescence intensity of the Hoechst-DNA conjugate decreases by nearly 100% upon subsequent titration of the Cu(I) complex, suggesting that the Cu(I) complex is able to release the Hoechst molecules from DNA minor groove into solvent solution after an exchange with them, which supports the view that the Cu(I) complex is DNA minor groove bin-

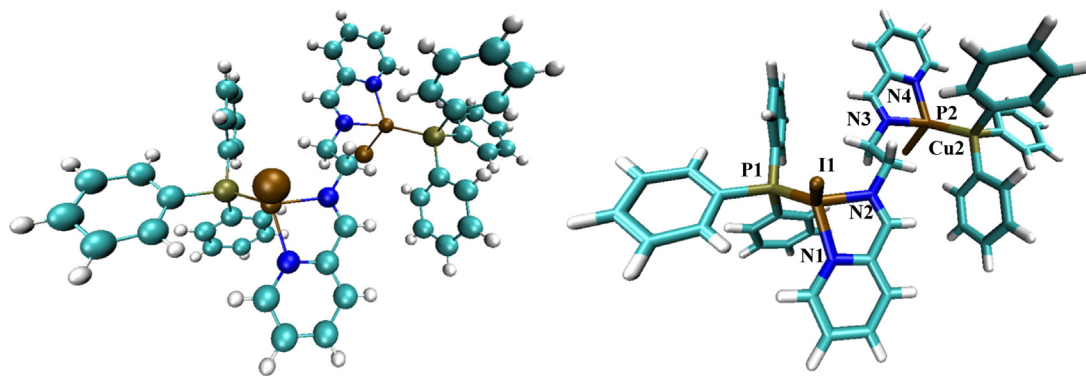


Fig. 1. The CPK and labeled licorice plots of the molecular structure of the Cu(I) complex  $[\text{Cu}(\text{PPh}_3)(\text{L}_{0.5})(\text{I})_2]$ .

Table 1

The crystal data and structure refinement parameters for the synthesized complex and the selected bond lengths (Å) and angles ( $^\circ$ ) around the metal center.

Empirical formula	$\text{C}_{50}\text{H}_{44}\text{Cu}_2\text{I}_2\text{N}_4\text{P}_2$	Bond (Å) / angle ( $^\circ$ )	
Formula weight (g/mol)	1143.71	Cu1–I1	2.5803(9)
Wavelength (Å)	1.54184	Cu1–P1	2.182(2)
T [K]	173.0	Cu1–N1	2.103(5)
Crystal system	Monoclinic	Cu1–N2	2.073(4)
Space group	$\text{P}2_1/\text{n}$	P1–Cu1–N1	115.0(1)
a [Å]	8.7424(2)	P1–Cu1–N2	125.4(1)
b [Å]	16.9780(6)	P1–Cu1–I1	124.02(5)
c [Å]	31.8558(10)	N1–Cu1–N2	79.7(2)
$\alpha$ [ $^\circ$ ]	90	N1–Cu1–I1	103.0(1)
$\beta$ [ $^\circ$ ]	91.434(3)	N2–Cu1–I1	99.8(1)
$\gamma$ [ $^\circ$ ]	90	Cu2–I2	2.6204(8)
V [Å <sup>3</sup> ]	4726.8(2)	Cu2–P2	2.193(1)
Z	4	Cu2–N3	2.097(4)
Density [g/cm <sup>3</sup> ]	1.607	Cu2–N4	2.092(4)
$\mu$ [mm <sup>-1</sup> ]	12.297	P2–Cu2–N3	125.4(1)
F(0 0 0)	2264.0	P2–Cu2–N4	122.1(1)
Crystal Size [mm]	$0.3 \times 0.03 \times 0.03$	P2–Cu2–I2	120.30(5)
Reflections collected	26,539	N3–Cu2–N4	79.1(2)
R <sub>int</sub> [%]	0.0538	N3–Cu2–I2	93.1(1)
Goodness-of-fit on F <sup>2</sup>	1.029	N4–Cu2–I2	107.4(1)

Computer programs: CrysAlis PRO [40], SHELXT [41], SHELXL2014 [42] and OlexSys [43].

der at A-T rich sequences, where the Hoechst molecule was located, as similarly reported for groove binder macrocyclic Cu(II) complex [56].

Another kind of competitive assay based on the MB probe was performed to prove the existence of intercalation mode. The emission spectra of MB–DNA conjugate were recorded before and after

adding the Cu(I) complex (Fig. 3B). Based on the results, the emission intensity of MB–DNA showed gradual enhancement up to 69.4% by increasing the Cu(I) complex concentration. So, it can be concluded that an exchange between the Cu(I) complex and methylene blue bonded to DNA took place, indicating an intercalative kind of binding. Similarly, recovery of MB fluorescence was attributed to an intercalation binding mode of curcumin Cu(II) complex [57].

### 3.2.3. Circular dichroism study

To obtain more information about the possible portion conformational changes related to the binding of the Cu(I) complex to specific DNA sites, the CD experiment was carried out. The CD spectrum of DNA in the typical B conformation exhibits a positive band at around 275 nm, which arises from base stacking and a negative band at around 245 nm due to right-handed helicity [58]. As regards, any specific conversion of DNA morphology sensitizes the CD signal, accordingly, the CD spectropolarimetry provides unique possibilities to identify and interpret DNA binding modes of small molecules with high sensitivity. Considering this, the CD spectra of CT–DNA were monitored in the absence and presence of the Cu(I) complex. It can be viewed that the presence of the Cu(I) complex caused a considerable increase in the intensity of positive peak than negative one without any significant change in the band positions (Fig. 4).

The enhancement of the positive CD band can offer typical intercalation including  $\pi$ -stacking and stabilization of the right-handed B form of DNA [59,60]. The observed increase in the negative CD peak of DNA can be due to partial intercalation of planer phenyl rings moieties between the base pairs in the minor groove

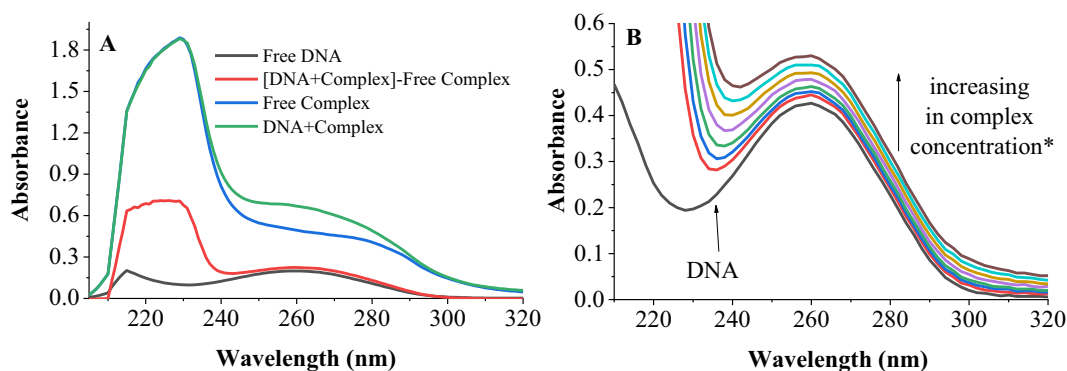
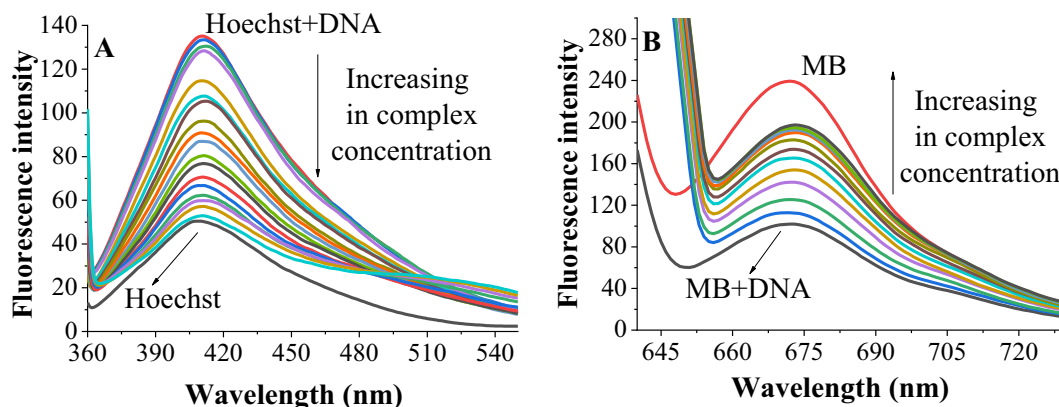
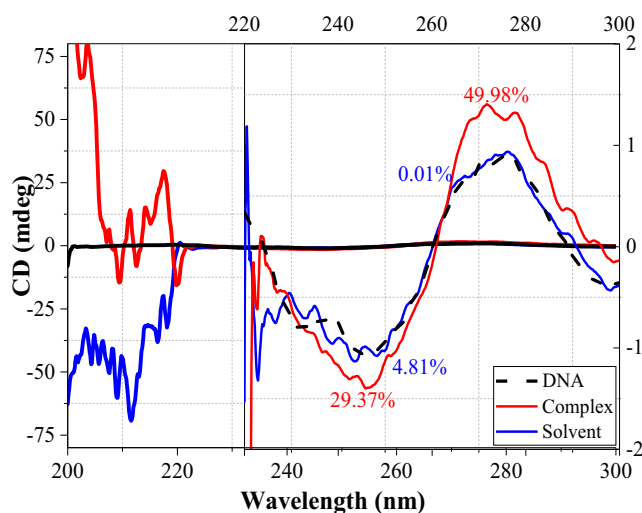


Fig. 2. (A) UV–Visible absorption spectra of the Cu(I) complex ( $1.74 \times 10^{-5}$  mol/L) in the absence and presence of DNA ( $3.02 \times 10^{-5}$  mol/L), (B) UV–Visible absorption spectra of  $1.45 \times 10^{-5}$  mol/L DNA by increasing the concentration of the complex from 0 to  $4.69 \times 10^{-6}$  mol/L up to 7 increments in 50 mmol/L Tris–HCl buffer (pH 7.4) at room temperature. \*All spectra are reported after removing the Cu(I) complex disturbance.



**Fig. 3.** (A) Competitive displacement analysis between the Cu(I) complex and Hoechst33258 in a pre-treatment Hoechst-DNA conjugate ( $C_{\text{Hoechst}} = 5 \times 10^{-6}$  mol/L,  $C_{\text{DNA}} = 1.18 \times 10^{-3}$  mol/L,  $C_{\text{complex}} = 0$  to  $1.12 \times 10^{-4}$  mol/L) in 50 mmol/L Tris HCl buffer (pH 7.4) at 288 K (B) Competitive displacement analysis between the complex and MB in a pre-treatment MB-DNA conjugate ( $C_{\text{MB}} = 5 \times 10^{-6}$  mol/L,  $C_{\text{DNA}} = 1.96 \times 10^{-4}$  mol/L,  $C_{\text{complex}} = 0$  to  $2.33 \times 10^{-4}$  mol/L) in 50 mmol/L Tris-HCl buffer (pH 7.4) at 288 K.



**Fig. 4.** The CD spectra of the interaction of  $1.81 \times 10^{-6}$  mol/L complex with  $2.15 \times 10^{-5}$  mol/L DNA.

and cause the release of the water from the grooves consequently the DNA helix can potentially tolerate more bending in the presence of the Cu(I) complex [61,62]. In overall, the changes in the CD spectra indicated that the binding of the Cu(I) complex to DNA caused stabilization of the right-handed B-DNA without any transition in form (B-DNA to A or Z form) [63,64]. Similarly, in the case of  $[\text{Cu}(\text{Cur})(\text{DIP})]^{+2}$ , the increased intensity of the both negative and positive bands indicated fixating the right-handed B conformation of CT-DNA via intercalation binding mode [57]. The effect of the solvent (DMSO 0.05%, Ethanol 0.1%) on the DNA structure was also investigated. As illustrated in Fig. 4, no significant change in the intrinsic CD spectrum of the DNA was observed, which indicated that the solvent does not disturb the DNA structure.

### 3.2.4. Steady-state fluorescence studies

To provide a detailed analysis of the interaction mechanism, thermodynamic parameters, and critical forces in the binding process, a steady state fluorescence experiment was utilized. Regarding the negligible fluorescence emission of both DNA helix and the Cu(I) complex, a fixed amount of Hoechst 33,258 was used to probe the interaction. Fig. 5A, B, C and D show the fluorescence emission of Hoechst-labeled DNA with increasing of the Cu(I) complex con-

centration at 288, 293, 298, and 303 K. Subsequent quenching of the probe-DNA conjugate with the sequential addition of the Cu(I) complex is considered as a direct approval for the interaction of the Cu(I) complex with DNA helix [65]. The observed fluorescence quenching does not show any significant change in the peak position. Stern–Volmer equation (Eq. (4)) was applied to evaluate the fluorescence quenching mechanism at a quantitative level [66,67]:

$$F_0/F = 1 + k_q \tau_0 [Q] = 1 + K_{SV} [Q] \quad (4)$$

where the Stern–Volmer quenching constant is described by  $K_{SV}$ , the apparent bimolecular quenching rate constant is defining by  $k_q$ ,  $[Q]$  is the concentration of the quencher complex and  $\tau_0$  the unquenched fluorophore average lifetime which is about  $1 \times 10^{-8}$  S [68]. Applying different temperatures (288, 293, 298, and 303 K) to eviscerate the Stern–Volmer plot, yields the  $K_{SV}$  values at a fixed y-axis intercept of 1 from the slop (Fig. 5E). The obtained Stern–Volmer constants at applied temperatures found to be in the range of  $14.04\text{--}6.44 \times 10^3 \text{ M}^{-1}$  that is along with the groove binding mode of the interaction [69]. The static or dynamic nature of the quenching mechanism can be distinguished by their dependence on temperature. Because an increase in temperature results in a larger diffusion coefficient and promotes electron transfer, the Stern–Volmer quenching constant becomes larger as the temperature goes up, implying a dynamic quenching mechanism. In contrast, in the case of a static mechanism, the thermal stability of the fluorophore–quencher complex decrease with increasing temperature, thus, the values of the Stern–Volmer quenching constants are expected to be smaller. The interaction of the Cu(I) complex with DNA leads to a significant decrease in  $K_{SV}$  values to 54.09% as temperature goes up to 303 K, supporting the involvement of static mechanism in the quenching process, as reported for interaction mechanism of a series of binary Cu(II) complexes containing intercalating ligand [70].

### 3.2.5. Binding equilibrium

The binding constant ( $K_b$ ) and the Hill coefficient ( $n$ ) for the interaction of the Cu(I) complex with DNA were calculated via the logarithmic Hill equation (Eq. (5)) (Fig. 5F) [71]:

$$\text{Log} \left( \frac{F_0 - F}{F} \right) = \text{Log} K_b + n \text{Log} [Q] \quad (5)$$

where  $F_0$  and  $F$  represent the fluorescence intensity of the Hoechst-labeled DNA in the absence and the presence of different the Cu(I) complex concentrations  $[Q]$ ,  $n$  is the Hill cooperativity coefficient to describe DNA binding sites cooperativity to put the Cu(I) complex

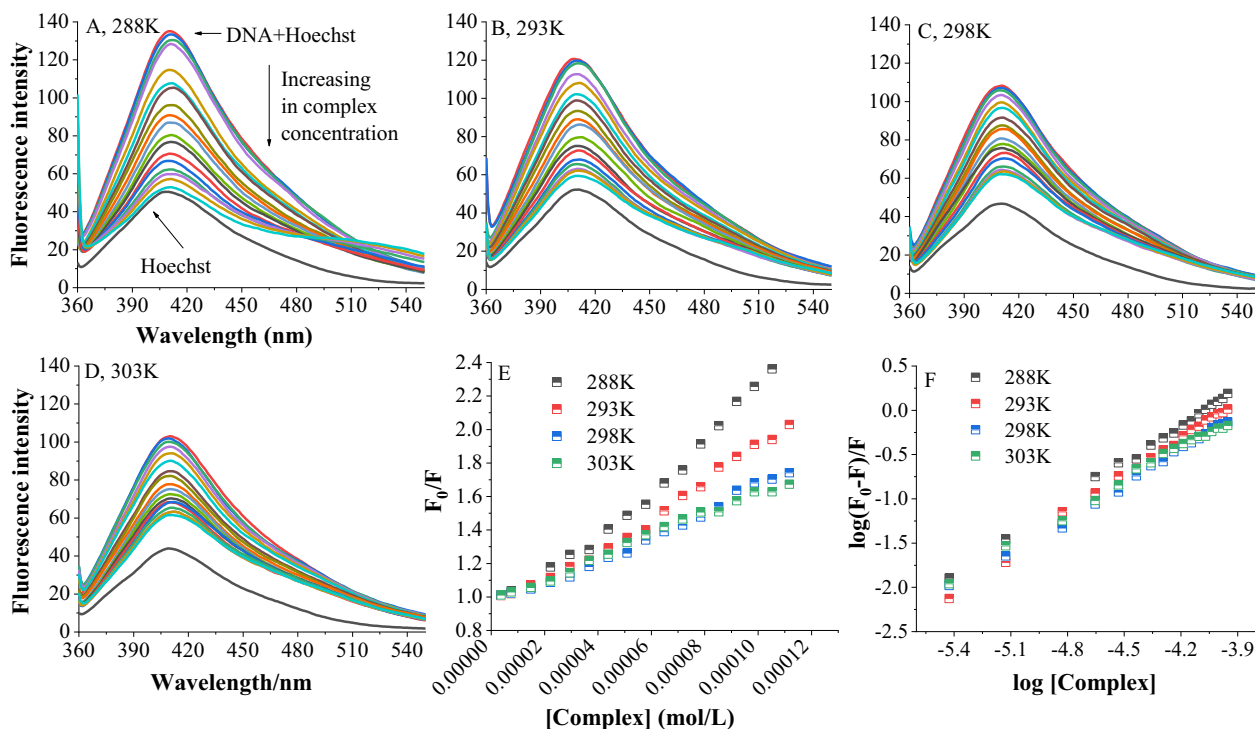


**Fig. 5.** **A, B, C, and D)** Fluorescence emission spectra of  $5 \times 10^{-6}$  mol/L and  $1.18 \times 10^{-3}$  mol/L of Hoechst and CT-DNA along with the Cu(I) complex concentration increasing from 0.0 to  $1.12 \times 10^{-4}$  mol/L in 50 mmol/L Tris-HCl buffer (pH 7.4) at 288, 293, 298, and 303, respectively. **(E)** Stern-Volmer plot of the Cu(I) complex-DNA interaction by applying temperatures 288, 293, 298, and 303 K, **(F)**  $\log(F_0-F)/F$  vs.  $\log[\text{Complex}]$  plot for the determination of binding constants corresponding to 288, 293, 298, and 303 K.

in these sites, and  $K_b$  (binding constant) utilizes DNA binding affinity of the Cu(I) complex. The calculated  $K_b$  and  $n$  are presented in Table 2. The downward trend of the Hill coefficient with temperature increasing, showing a negative cooperation effect. Additionally, the  $K_b$  values decrease as temperature rises, suggesting that static quenching occurs [34].

### 3.2.6. Thermodynamic parameters

Intermolecular forces that exist between small ligands and biomolecules can be based on four types of non-covalent interactions i.e. hydrogen bond, van der Waals force, electrostatic interaction, and hydrophobic force [72]. According to the data of enthalpy changes ( $\Delta H$ ) and entropy changes ( $\Delta S$ ), the model of interaction between ligand and biomolecule can be concluded: (1)  $\Delta H > 0$  and  $\Delta S > 0$ , hydrophobic forces; (2)  $\Delta H < 0$  and  $\Delta S < 0$ , van der Waals interactions and hydrogen bonds; (3)  $\Delta H < 0$  and  $\Delta S > 0$ , electrostatic interactions [73,74]. To identify the main interaction force between DNA and the Cu(I) complex, the thermodynamic parameters were derived using the Gibbs-Helmholtz equation (Eq. (6)) [75]:

$$\Delta G^\circ = \Delta H^\circ - T\Delta S^\circ = -RT \ln K_b \quad (6)$$

where  $K_b$  is the binding constant at the corresponding temperature,  $\Delta G^\circ$  shows the free energy change for the binding reaction,  $\Delta H^\circ$  represents the molar enthalpy change, the molar entropy change is defined by  $\Delta S^\circ$ ,  $R = 1.9872 \text{ cal mol}^{-1} \text{ K}^{-1}$  is the universal gas constant, and  $T$  is the temperature in kelvins. The corresponding thermodynamic parameters,  $\Delta G^\circ$ ,  $\Delta H^\circ$ , and  $\Delta S^\circ$ , were reported in Table 3. The negative binding free energies ( $\Delta G^\circ$ ) evidenced favorable interactions between the Cu(I) complex and DNA [47]. The significant volume reduction of the Cu(I) complex-DNA conjugate in the intercalation binding mode or the changes in solvation during the interaction process can be reflected in negative  $\Delta S^\circ$  value. Based on the negative value of  $\Delta H^\circ$ , binding of the Cu(I) complex to DNA is

**Table 2**

The binding parameters for the Cu(I) complex-DNA interaction.

T (K)	$K_b$ ( $\text{L mol}^{-1}$ )	$n$	$R^2$
288	$8.06 \times 10^5$	1.45	0.9844
293	$4.85 \times 10^5$	1.43	0.9953
298	$1.59 \times 10^5$	1.34	0.9972
303	$4.62 \times 10^4$	1.21	0.9915

**Table 3**

The thermodynamic parameters for the Cu(I) complex-CT-DNA interaction.

T(K)	$\Delta G$ ( $\text{kcal mol}^{-1}$ )	$\Delta S$ ( $\text{cal mol}^{-1} \text{ K}^{-1}$ )	$\Delta H$ ( $\text{kcal mol}^{-1}$ )
288	-7.78	-89.20	-33.59
293	-7.62		
298	-7.09		
303	-6.47		

an exothermic reaction, which means that higher temperatures lead to instability of the Cu(I) complex-DNA conjugate, confirmed by the decrease in  $K_b$  values as temperature increases [76]. According to Ross and Subramanian studies [73], the negative values of  $\Delta H^\circ$  and  $\Delta S^\circ$  are indicated of most probable the van der Waals interactions as main driving forces in the Cu(I) complex binding to DNA which is the main evidence for intercalation binding mode as reported for the DNA interaction of pyrazoline based palladium(II) complexes [27] and macrocyclic Cu(II) complex [56].

### 3.2.7. Molecular docking studies

Based on the competitive fluorescence studies, the Cu(I) complex is able to release the Hoechst molecules from DNA minor groove at A-T rich region as well as MB from two DNA strands. To confirm the experimental results, molecular docking simulation was performed with DNA sequence CGCGAATTCGCG/CGCGAATTCGCG (PDB ID: 1g3x), which contains A-T bases in the

middle part (minor groove), where the Cu(I) complex is probably bonded. From the docking analysis, the best conformer with the lowest binding energy was picked from the 20 unique conformations among 500 runs (Fig. 6).

The selected docking pose showed that the Cu(I) complex can bind to DNA model with high affinity ( $-7.4$  kcal/mol). From Fig. 6, it is clear that the planar aromatic rings of the Cu(I) complex was inserted in the core of the adenine DA606 and adenine DA605 nucleobases at the middle part of DNA composed by AT base pairs through  $\pi$ - $\pi$  stacking interactions in  $4.54$  Å and  $5.19$  Å, while the remaining part of the Cu(I) complex lies in DNA minor groove between DT619 to DA605. Dock results also show the presence of weak hydrophobic forces in the interaction (Fig. 7). The obtained results confirm the role of both intercalation ( $\pi$ - $\pi$  interactions between the bases) and groove binding at A-T rich region in the interaction and the experiments results accuracy.

### 3.2.8. Cytotoxicity evaluation

The results of cytotoxicity evaluation of the Cu(I) complex and cisplatin on MCF-7 cancer cells and HUVEC normal cells has been shown in Table 4. As we can see the toxicity of the Cu(I) complex toward MCF-7 cells was higher than cisplatin at all concentrations. According to the findings, the highest descent in MCF-7 cells viability reached to 21% by  $160$   $\mu$ g/mL of the Cu(I) complex while

cisplatin showed a 39% reduction in cells viability at the same concentration, which proved more positive effect of the Cu(I) complex on inhibition of cancer cell proliferation. Based on the published data, cytotoxic mechanism of copper complexes is different than that of platinum complexes [77–79], which is mainly related to the copper affinity for binding to sites occupied by other metals, and or their ability for DNA intercalation [13,21,80]. So, it can be concluded that the more cytotoxicity effect of the complex is attributed to DNA intercalation binding mode and lipophilic character, as reported for copper(I)-phosphine polypyridyl complexes [20].

On the other hand, it can be clearly seen in Table 4 that the HUVEC cell viability percent was higher than MCF-7 at all the Cu(I) complex concentrations, that is indicated the Cu(I) complex was more sensitive to inhibition of cancer cells than normal cells. This is consistent with in vitro cell culture experiments that demonstrated a significant antiproliferative activity for Cu(I) compounds against several cancer cell lines with a preferential cell growth inhibition towards tumour than nonmalignant cells [81]. Moreover, other studies showed that some binuclear copper-based complexes can remarkably induce apoptosis and inhibit angiogenesis to mediate tumour growth [82].

In addition, to determine apoptosis effects of the Cu(I) complex and cisplatin on MCF-7 and HUVEC cell lines, morphological assay of

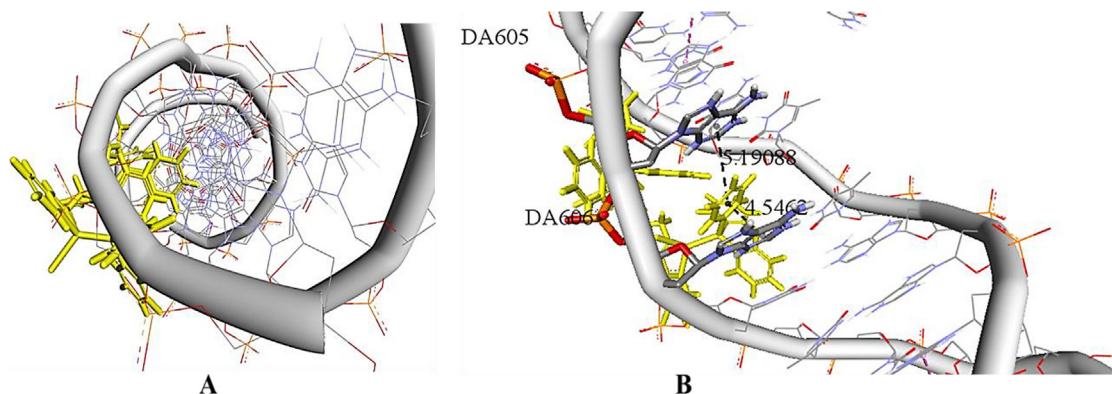


Fig. 6. (A) Molecular modeling of the interaction between the Cu(I) complex and DNA dodecamer d(CGCGAATTCGCG/CGCGAATTCGCG) in a box with the number of grid points in  $x \times y \times z$  directions,  $20 \times 40 \times 20$  and a grid spacing of  $1.00$  Å. (B) The  $\pi$ - $\pi$  stacking distance between the Cu(I) complex and DNA nucleobases.

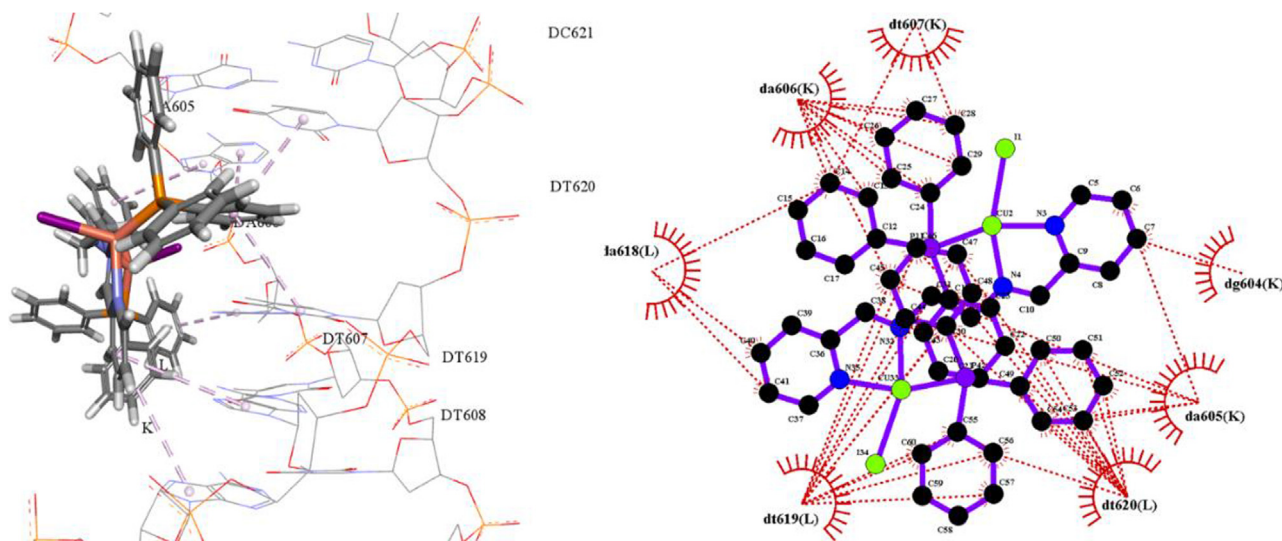
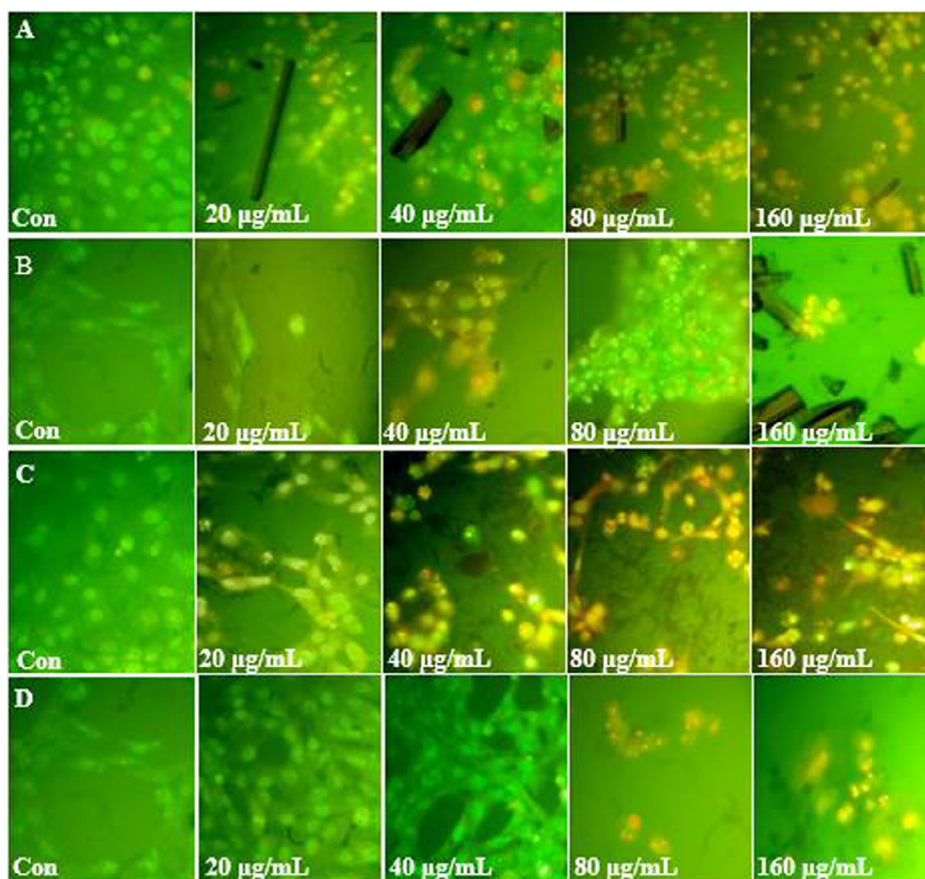


Fig. 7. The involvement of hydrophobic and van der Waals forces in the interaction of the Cu(I) complex and DNA model.

**Table 4**  
MCF-7 and HUVEC cell viability percent in the presence of the Cu(I) complex on 72 h incubation.

Concentration	% Viable MCF-7 cancer cells		% Viable HUVEC cells	
	Cu(I) complex	Cisplatin	Cu(I) complex	Cisplatin
20 µg/mL	49.59 ± 4.60	61.83 ± 3.10	69.95 ± 3.64	104.36 ± 9.87
40 µg/mL	34.11 ± 2.31	55.02 ± 0.50	48.04 ± 1.03	69.13 ± 4.40
80 µg/mL	27.15 ± 1.02	49.34 ± 5.70	34.97 ± 2.09	34.24 ± 3.40
160 µg/mL	21.35 ± 0.50	39.33 ± 1.45	23.43 ± 0.79	28.40 ± 0.56



**Fig. 8.** Ethidium bromide-Acridine orange staining of MCF-7 (A, C) and HUVEC cells (B, D) treated 72 h with different concentrations of the Cu(I) complex and cisplatin.

cell death was investigated using acridin orange-ethidium bromide dye staining. The cytotoxic activities of these compounds in their induction of early and late apoptosis were analysed in a concentration dependent manner. 72 h after treatment different morphological features like bright green early apoptotic cells with nuclear margination and chromatin condensation were observed in all cell lines, while nuclear morphology from control cells were seen uniformly green with normal morphology (Fig. 8). As the concentration of the Cu(I) complex and cisplatin increased, orange stained cells which show high levels of apoptotic cell death became more than bright green nucleus. The results clearly showed the Cu(I) complex and cisplatin were able to induce apoptosis in MCF-7 cancer cells more than HUVEC normal cells.

#### 4. Conclusion

The monoclinic phase  $[\text{Cu}(\text{PPh}_3)(\text{L}_{0.5})(\text{I})_2]$  with a tetrahedral geometry was identified by X-ray single-crystal diffraction data. The  $\pi$ - $\pi$  stacking interaction between the DNA base pairs and the

aromatic chromophores of the Cu(I) complex results in DNA strand separation which recognize by hyperchromism in UV-Visible spectra. A decrease in the fluorescence intensity of Hoechst-DNA conjugate and an increase in the emission intensity of MB-DNA system, confirmed that the Cu(I) complex was able to displace both Hoechst molecules from the minor groove of DNA helix at A-T rich region and MB dye from the intercalative binding sites. A gradual decrease in  $K_{SV}$  value by temperature increases indicated static fluorescence quenching involvement in the binding process. Based on the thermodynamic data (negative  $\Delta H$  and  $\Delta S$  values) and molecular docking results van der Waals and hydrophobic forces play the key role in the binding of the Cu(I) complex to DNA. The increased intensity of the both negative and positive CD bands indicated binding of the Cu(I) complex to DNA caused stabilization of the right-handed B-DNA without any transition in form. The molecular docking simulations confirmed the role of both intercalation and groove binding in the interaction process and the accuracy of the experimental results. The cytotoxicity results on human breast cancer cells showed more anticancer effect of the Cu(I) complex

than cisplatin against MCF-7 cells and also the Cu(I) complex was more sensitive to inhibition of cancer cells than normal cells. The present study not only enable us to have a new viewpoint of the interaction mechanism of the Cu(I) complex with DNA, but also helps us to design new molecular models of novel and more efficient potential metallo drug which treated DNA.

## Funding

There are no funders from any person or institution to report for this submission.

## CRediT authorship contribution statement

**Nahid Shahabadi:** Supervision. **Farshad Shiri:** Investigation. **Saba Hadidi:** Investigation. **Kaveh Farshadfar:** Formal analysis. **Maryam Darbemamieh:** Investigation. **S. Mark Roe:** Formal analysis.

## Declaration of Competing Interest

The authors declare that they have no known competing financial interests or personal relationships that could have appeared to influence the work reported in this paper.

## Acknowledgments

We thank Inorganic Research Lab. 2 of Razi University.

## Appendix A. Supplementary material

Supplementary data to this article can be found online at <https://doi.org/10.1016/j.molliq.2021.116290>.

## References

- [1] H. Tapiero, D. Townsend, K. Tew, *Biomed. Pharmacother.* 57 (2003) 386.
- [2] F. Tisato, C. Marzano, M. Porchia, M. Pellei, C. Santini, *Med. Res. Rev.* 30 (2010) 708.
- [3] M.C. Linder, M. Hazegh-Azam, *Am. J. Clin. Nutr.* 63 (1996) 797S.
- [4] S.A. Lowndes, A.L. Harris, *J. Mammary Gland Biol. Neoplasia* 10 (2005) 299.
- [5] M. Zowczak, M. Iskra, L. Torliński, S. Cofta, *Biol. Trace Elem. Res.* 82 (2001) 1.
- [6] S. Lowndes, A. Harris, *Oncol. Res. Featuring Preclinical Clin. Cancer Therap.* 14 (2004) 529.
- [7] G. Khan, S. Merajver, *Expert Opin. Invest. Drugs* 18 (2009) 541.
- [8] K. Camphausen, M. Sproull, S. Tantama, S. Sankineni, T. Scott, C. Menard, C.N. Coleman, M.W. Brechbiel, *Bioorg. Med. Chem.* 11 (2003) 4287.
- [9] K. Camphausen, M. Sproull, S. Tantama, V. Venditto, S. Sankineni, T. Scott, M.W. Brechbiel, *Bioorg. Med. Chem.* 12 (2004) 5133.
- [10] M. Porchia, A. Dolmella, V. Gandin, C. Marzano, M. Pellei, V. Peruzzo, F. Refosco, C. Santini, F. Tisato, *Eur. J. Med. Chem.* 59 (2013) 218.
- [11] V. Gandin, F. Tisato, A. Dolmella, M. Pellei, C. Santini, M. Giorgetti, C. Marzano, M. Porchia, *J. Med. Chem.* 57 (2014) 4745.
- [12] K.H. Mashat, B.A. Babgi, M.A. Hussien, M.N. Arshad, M.H. Abdellatif, *Polyhedron* 158 (2019) 164.
- [13] C. Marzano, V. Gandin, M. Pellei, D. Colavito, G. Papini, G.G. Lobbia, E. Del Giudice, M. Porchia, F. Tisato, C. Santini, *J. Med. Chem.* 51 (2008) 798.
- [14] V. Gandin, M. Pellei, F. Tisato, M. Porchia, C. Santini, C. Marzano, *J. Cell Mol. Med.* 16 (2012) 142.
- [15] A. Herbert, A. Rich, *Genetica* 106 (1999) 37.
- [16] A. Travers, G. Muskhelishvili, *FEBS J.* 282 (2015) 2279.
- [17] R.R. Sinden, *DNA structure and function*, Elsevier, 2012.
- [18] E.R. Jamieson, S.J. Lippard, *Chem. Rev.* 99 (1999) 2467.
- [19] K. Suntharalingam, O. Mendoza, A.A. Duarte, D.J. Mann, R. Vilar, *Metallomics* 5 (2013) 514.
- [20] W. Villarreal, L. Colina-Vegas, G. Visbal, O. Corona, R.S. Corrêa, J. Ellena, M.R. Cominetti, A.A. Batista, M. Navarro, *Inorg. Chem.* 56 (2017) 3781.
- [21] U.K. Komarnicka, R. Starosta, M. Plotek, R.F. de Almeida, M. Jezowska-Bojczuk, A. Kyzioł, *Dalton Trans.* 45 (2016) 5052.
- [22] R.A. Khan, M. Usman, R. Dhivya, P. Balaji, A. Alsalmeh, H. AlLohedan, F. Arjmand, K. AlFarhan, M.A. Akbarsha, F. Marchetti, *Sci. Rep.* 7 (2017) 45229.
- [23] N. Shahabadi, F. Shiri, S. Hadidi, K. Farshadfar, S. Sajadimajid, S.M. Roe, *Spectrochim. Acta Part A Mol. Biomol. Spectrosc.* (2020) 118280.
- [24] P.A. Vekariya, P.S. Karia, B.S. Bhatt, M.N. Patel, *J. Inorg. Organomet. Polym. Mater.* 28 (2018) 2749.
- [25] Y.-X. Mi, S. Wang, X.-X. Xu, H.-Q. Zhao, Z.-B. Zheng, X.-L. Zhao, *J. Chil. Chem. Soc.* 64 (2019) 4392.
- [26] D.-Y. Zhang, Y. Nie, H. Sang, J.-J. Suo, Z.-J. Li, W. Gu, J.-L. Tian, X. Liu, S.-P. Yan, *Inorg. Chim. Acta* 457 (2017) 7.
- [27] K.P. Thakor, M.V. Lunagariya, B.S. Bhatt, M.N. Patel, *Appl. Organomet. Chem.* 32 (2018) e4523.
- [28] J.M. Woynarowski, *Advances in DNA Sequence-Specific Agents*, Elsevier (2002) 1–27.
- [29] B.S. Bhatt, D.H. Gandhi, F.U. Vaidya, C. Pathak, T.N. Patel, *J. Biomol. Struct. Dyn.* (2020) 1.
- [30] N. Shahabadi, S. Hadidi, F. Shiri, *J. Biomol. Struct. Dyn.* 38 (2020) 283.
- [31] K. Gholivand, K. Farshadfar, S.M. Roe, M. Hosseini, A. Gholami, *CrystEngComm* 18 (2016) 7104.
- [32] K. Gholivand, R. Salami, K. Farshadfar, R.J. Butcher, *Polyhedron* 119 (2016) 267.
- [33] M. Abdoh, I. Warad, S. Naveen, N. Lokanath, R. Salghi, *Acta Crystallographica Section E: Crystallographic Communications* 71 (2015) o431.
- [34] N. Shahabadi, S. Hadidi, Z. Ghasemian, A.A. Taherpour, *Spectrochim. Acta Part A Mol. Biomol. Spectrosc.* 145 (2015) 540.
- [35] O. Trott, A.J. Olson, *J. Comput. Chem.* 31 (2010) 455.
- [36] G.M. Morris, R. Huey, W. Lindstrom, M.F. Sanner, R.K. Belew, D.S. Goodsell, A.J. Olson, *J. Comput. Chem.* 30 (2009) 2785.
- [37] R. Gaur, R.A. Khan, S. Tabassum, P. Shah, M.I. Siddiqi, L. Mishra, *J. Photochem. Photobiol., A* 220 (2011) 145.
- [38] L. Malinina, M. Soler-López, J. Aymami, J.A. Subirana, *Biochemistry* 41 (2002) 9341.
- [39] G.M. Morris, D.S. Goodsell, R.S. Halliday, R. Huey, W.E. Hart, R.K. Belew, A.J. Olson, *J. Comput. Chem.* 19 (1998) 1639.
- [40] P. CrysAlis, Yarnton, Oxfordshire, England, 2014.
- [41] G.M. Sheldrick, *Acta Crystallogr., Sect. A: Found. Adv* 70 (2014) C1437.
- [42] G.M. Sheldrick, *Acta Crystallogr. Sect. C: Struct. Chem.* 71 (2015) 3.
- [43] C.B. Hübschle, G.M. Sheldrick, B. Dittrich, *J. Appl. Crystallogr.* 44 (2011) 1281.
- [44] M.M. Ackerman, C. Ricciardi, D. Weiss, A. Chant, C.M. Kraemer-Chant, *J. Chem. Educ.* 93 (2016) 2089.
- [45] A. Pyle, J. Rehmann, R. Meshoyrer, C. Kumar, N. Turro, J.K. Barton, *J. Am. Chem. Soc.* 111 (1989) 3051.
- [46] G. Prati, J. Bernadou, B. Meunier, *Adv. Inorganic Chem., Elsevier* (1998) 251–312.
- [47] N. Shahabadi, S. Hadidi, *Spectrochim. Acta Part A Mol. Biomol. Spectrosc.* 96 (2012) 278.
- [48] P. Kumar, R.J. Butcher, A.K. Patra, *Inorg. Chim. Acta* 506 (2020) 119532.
- [49] P. Ding, Y. Wang, H. Kou, J. Li, B. Shi, *J. Mol. Struct.* 1196 (2019) 836.
- [50] L. Zarei, Z. Asadi, M. Dusek, V. Eigner, *J. Photochem. Photobiol., A* 374 (2019) 145.
- [51] P. Ghorai, R. Saha, S. Bhuiya, S. Das, P. Brandão, D. Ghosh, T. Bhaumik, P. Bandyopadhyay, D. Chattopadhyay, A. Saha, *Polyhedron* 141 (2018) 153.
- [52] N. Shahabadi, S. Hadidi, A.A. Taherpour, *Appl. Biochem. Biotechnol.* 172 (2014) 2436.
- [53] P. Vardevanyan, A. Antonyan, M. Parsadanyan, M. Shahinyan, L. Hambardzumyan, *J. Appl. Spectrosc.* 80 (2013) 595.
- [54] E.T. Wahyuni, D.H. Tjahjono, N. Yoshioka, H. Inoue, *Spectrochim. Acta Part A Mol. Biomol. Spectrosc.* 77 (2010) 528.
- [55] M.C. Vega, I. García Sáez, J. Aymami, R. Eritja, G.A. Van Der Marel, J.H. Van Boom, A. Rich, M. Coll, *Eur. J. Biochem.* 222 (1994) 721.
- [56] N. Shahabadi, M. Hakimi, T. Morovati, N. Fatahi, *Nucleosides Nucleotides Nucleic Acids* 36 (2017) 497.
- [57] N. Shahabadi, M. Falsafi, N.H. Moghadam, *J. Photochem. Photobiol., B* 122 (2013) 45.
- [58] D.M. Gray, R.L. Ratliff, M.R. Vaughan, *Methods in enzymology*, Elsevier (1992) 389–406.
- [59] A. Dar, A.M. Shamsuzzaman, M. Gattoo, *J. Biomol. Res. Ther* 4 (2015) 2.
- [60] B. Nordén, F. Tjernereld, *Biopolymers: Original Research on Biomolecules* 21 (1982) 1713.
- [61] S. Das, G.S. Kumar, *J. Mol. Struct.* 872 (2008) 56.
- [62] M. Kumar, M. Kaushik, S. Chaudhary, S. Kukreti, *J. Drug Metab. Toxicol.* 7 (2016) 1.
- [63] N. Shahabadi, S. Mohammadi, *Bioinorg. Chem. Appl.* 2012 (2012).
- [64] T. Das, S.K. Kuttly, R. Tavallaie, A.I. Ibugo, J. Panchoompo, S. Sehar, L. Aldous, A. W. Yeung, S.R. Thomas, N. Kumar, *Sci. Rep.* 5 (2015) 8398.
- [65] H.-Y. Zou, H.-L. Wu, Y. Zhang, S.-F. Li, J.-F. Nie, H.-Y. Fu, R.-Q. Yu, *Journal of fluorescence* 19 (2009) 955.
- [66] K. Ali, F. Abul Qais, S. Dwivedi, E.M. Abdel-Salam, S.M. Ansari, Q. Saquib, M. Faisal, A.A. Al-Khedhairi, M. Al-Shaeri, J. Musarrat, *J. Biomol. Struct. Dyn.* 36 (2018) 2530.
- [67] E. Perianu, I. Rau, L.E. Vijan, *Spectrochim. Acta Part A Mol. Biomol. Spectrosc.* 206 (2019) 8.
- [68] Y. Sun, S. Bi, D. Song, C. Qiao, D. Mu, H. Zhang, *Sens. Actuators, B* 129 (2008) 799.
- [69] C.V. Kumar, E.H. Punzalan, W.B. Tan, *Tetrahedron* 56 (2000) 7027.
- [70] D. İnci, R. Aydın, Ö. Vatan, Y. Zorlu, N. Çinkilç, *J. Biomol. Struct. Dyn.* 36 (2018) 3878.
- [71] N. Shahabadi, F. Shiri, S. Hadidi, *Spectrochim. Acta Part A Mol. Biomol. Spectrosc.* 219 (2019) 195.
- [72] N. Shahabadi, F. Shiri, *Nucleos. Nucleot. Nucleic Acids* 36 (2017) 83.
- [73] P.D. Ross, S. Subramanian, *Biochemistry* 20 (1981) 3096.

- [74] D. Naik, P. Moorthy, K. Priyadarsini, *Chem. Phys. Lett.* 168 (1990) 533.
- [75] N. Shahabadi, F. Shiri, M. Norouzibazaz, A. Falah, *Nucleosides Nucleotides Nucleic Acids* 37 (2018) 125.
- [76] N. Shahabadi, S. Hadidi, *Spectrochim. Acta Part A Mol. Biomol. Spectrosc.* 122 (2014) 100.
- [77] C. Santini, M. Pellei, V. Gandin, M. Porchia, F. Tisato, C. Marzano, *Chem. Rev.* 114 (2014) 815.
- [78] X. Wang, Z. Guo, *Chem. Soc. Rev.* 42 (2013) 202.
- [79] N.J. Wheate, S. Walker, G.E. Craig, R. Oun, *Dalton Trans.* 39 (2010) 8113.
- [80] C. Santini, M. Pellei, G. Papini, B. Morresi, R. Galassi, S. Ricci, F. Tisato, M. Porchia, M.P. Rigobello, V. Gandin, *J. Inorg. Biochem.* 105 (2011) 232.
- [81] V. Gandin, A. Trenti, M. Porchia, F. Tisato, M. Giorgetti, I. Zanusso, L. Trevisi, C. Marzano, *Metallomics* 7 (2015) 1497.
- [82] X.Y. Qin, L.C. Yang, F.L. Le, Q.Q. Yu, D.D. Sun, Y.N. Liu, J. Liu, *Dalton Trans.* 42 (2013) 14681.